Inhomogeneity effects in oxygen-doped $HgBa_2CuO_4$

C. Ambrosch-Draxl[1,2,*] and E. Ya. Sherman[3]
[1]*Institute for Physics, University Graz, Universitätsplatz 5, A-8010 Graz, Austria*
[2]*Chair of Atomistic Modelling and Design of Materials, University Leoben, Erzherzog-Johann-Straße 3, A-8700 Leoben, Austria*
[3]*Department of Physics, University of Toronto, 60 St. George Street, Toronto, Ontario M5S 1A7, Canada*
(Received 25 January 2006; revised manuscript received 17 May 2006; published 6 July 2006)

We theoretically investigate inhomogeneity effects on the charges, electric field gradients, and site-projected densities of states in $HgBa_2CuO_{4+\delta}$. We find pronounced differences in the doping-induced number of holes at different atomic sites. The contributions of these sites to the density of states in the vicinity of the Fermi level are peaked at the same energy, but vary in magnitude by up to 70% and have a different energy dependence. Due to this energy dependence the role of the intrinsic inhomogeneities for superconductivity strongly depends on the energy and character of the quasiparticle mediating the Cooper pairing. Our results can explain the origin of doping-induced effects observed either by local or macroscopic experimental probes.

DOI: 10.1103/PhysRevB.74.024503 PACS number(s): 74.81.−g, 74.25.Jb, 74.72.−h

I. INTRODUCTION

Doping is the most crucial parameter to influence the critical temperature in high-T_c cuprates. The metallic state is reached by doping through the replacement of ions or by an introduction of excess oxygen. Thereby the dopant adds states at the Fermi level E_F, where these new charge carriers (holes) cause a downward shift of E_F and the carrier concentration in the CuO_2 planes is changed.

Among all doped single-layer cuprates, $HgBa_2CuO_{4+\delta}$ shows the highest T_c close to 94 K.[1] This fact as well as the pressure dependence of T_c in this family of the superconducting cuprates, stimulated the studies of their electron band structure within density functional theory (DFT). Early calculations helped to understand the properties of undoped single-layer[2] and multilayer[3] compounds. In addition, they demonstrated the importance of the proximity of the Fermi level to the van Hove singularity in the electron spectra of CuO_2 planes,[4] which can be achieved by applying pressure and/or by doping. The band structure and the bonding character of the dopant oxygen to the nearest Hg ion was investigated for $\delta=0.5$ in the doped three-layer compound $HgBa_2Ca_2Cu_3O_{8+\delta}$ by supercell calculations.[5]

At present, most of the theoretical models make use of two simplifications to describe doping effects in the complex physics of these systems: First, they use the carrier concentration rather than the doping level as an input parameter, and second, they assume that the additional charge is uniformly distributed within the different sites of the same atomic species in the CuO_2 plane. Concerning the former point, it has been shown[6] for $HgBa_2CuO_{4+\delta}$ how doping influences the charge carrier distribution and what limits the amount of holes that can be created. For the latter point, no first-principles calculations have been performed for any of the cuprates.

At the same time there is strong experimental evidence for intrinsic inhomogeneous charge distribution in high-T_c compounds. For example, the existence of stripes[8] in underdoped La_2CuO_4 and Bi based compounds is a clear manifestation of this. However, there are other sources of spatially nonuniform charge density. Scanning tunneling microscopy experiments performed on $Bi_2Sr_2CaCu_2O_{8+x}$ exhibit an inhomogeneous surface carrier distribution on a length scale of 14 Å, in the normal as well as in the superconducting state.[9] It was claimed that this inhomogeneity has an unknown origin but is an intrinsic property of this doped material, i.e., not related to impurities. More recently, it was found that the nanoscale electronic disorder in cuprates can be traced back to inhomogeneities on the atomic scale.[10] Local bulk probes such as nuclear quadrupole resonance (NQR) and nuclear magnetic resonance (NMR) experiments exhibit not only changes in the hole content with doping, but also the existence of different sites of the same species as it was seen in Tl-based compounds[11] and Sr doped La_2CuO_4.[12]

Since the spatial scale of inhomogeneities is determined by the amount of dopants, for doping levels in the regime of underdoped to optimally doped, investigations on a scale of a few lattice parameters are required. Wang *et al.* considered the role of the Coulomb impurities located close to the CuO_2 plane on the spatial dependence of the gap in a *d*-wave superconductor within the *t*-*J* model.[13] In this work, we perform parameter-free calculations which allow a detailed analysis of the charge distribution. By this way the inhomogeneities can be quantitatively studied and linked to experimental findings. We investigate the doping-induced charge redistribution in the $HgBa_2CuO_{4+\delta}$ compound. Focusing on the CuO_2 planes, we will show that the inhomogeneity is quite pronounced, it occurs on a scale of a few lattice constants, and is strongly doping dependent. We will also consider the consequences for the site-projected densities of states and their impact on superconductivity. To this extent, we have performed a series of supercell calculations corresponding to oxygen concentrations of $\delta=\frac{1}{8}$, $\frac{1}{6}$, $\frac{2}{9}$, and $\frac{1}{4}$.

II. SUPERCELL CALCULATIONS

Unit cells of the eightfold, sixfold, ninefold, and fourfold size compared to the undoped case are presented in Fig. 1. The particular environment with respect to the dopant makes the various copper and oxygen sites within the CuO_2 planes inequivalent. The coordinates of these different types of Cu and O atoms are provided in Table I for the structures shown

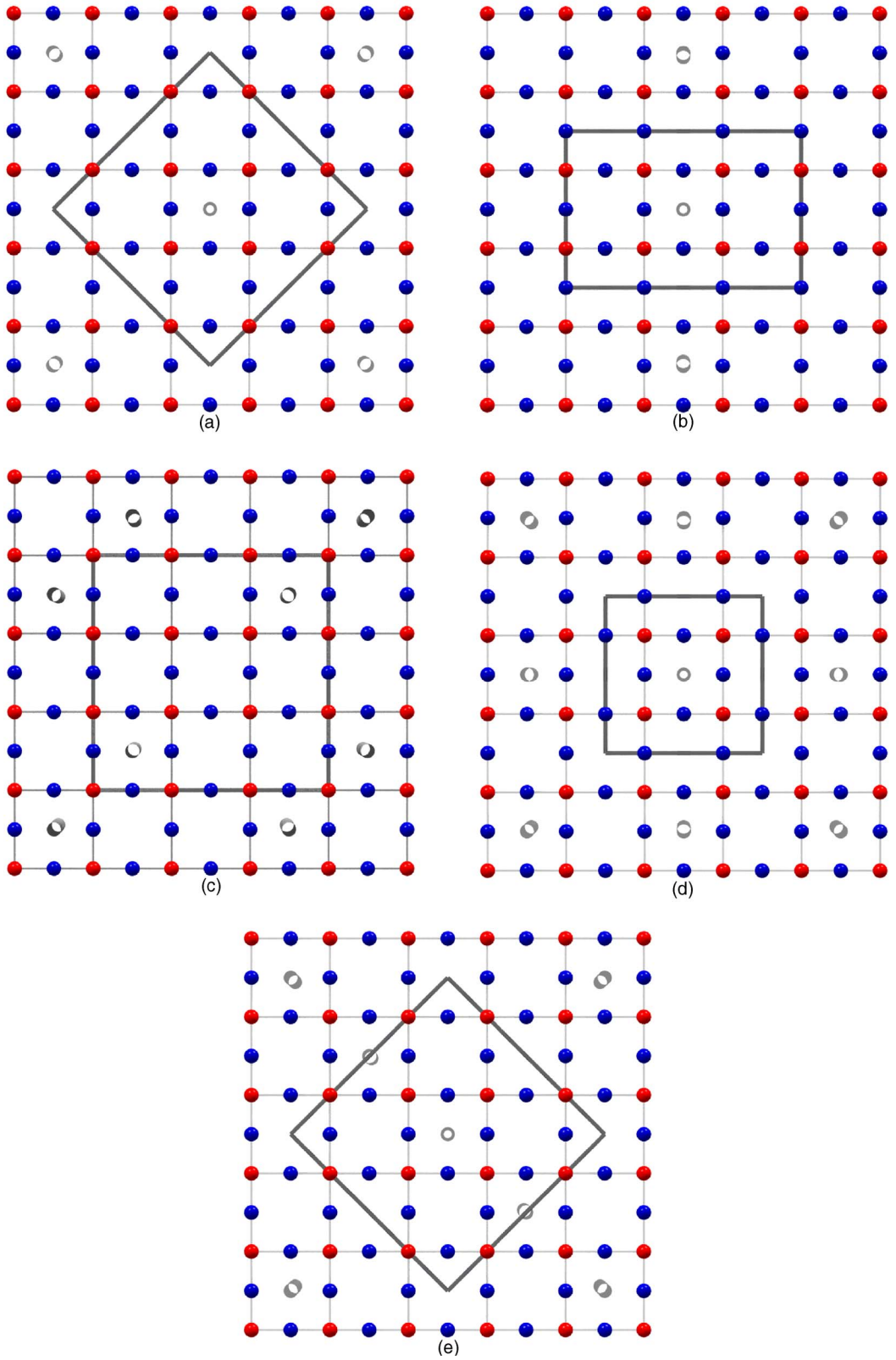

FIG. 1. (Color online) Copper-oxygen planes of the $HgBa_2CuO_{4+\delta}$ supercells representing the doping concentrations of δ=0.125 (upper left panel), 0.167 (upper right panel), 0.22 (lower left panel), and 0.25 (lower right panel). The unit cells are indicated by the bold gray lines, the copper (oxygen) atoms by the red (blue) spheres. The projection of the dopant oxygen (located at the Hg plane) onto these planes is marked by the gray circles. In the lowest panel, an alternative structure for δ=0.25 is displayed.

TABLE I. Copper and oxygen types, their multiplicities (in parentheses), their (X,Y) coordinates given in lattice constants A and B of the respective supercells, and their in-plane distances to the nearest dopant oxygen d_O, where a is the single cell lattice parameter. h_s denotes the number of holes created by doping at the given site, $V_{\gamma\gamma}$ are the diagonal components of the electric field gradient tensor in 10^{21} V/m^2 units, and η is the corresponding asymmetry parameter. The principal axes of the EFG are either identical or close to the crystal axes.

Doping	Ion	X	Y	d_O	h_s [e]	V_{11}	V_{22}	V_{33}	η
0.125	Cu1 (4)	$\frac{1}{4}$	0	$a\sqrt{10}/2$	0.0515	2.6	2.6	−5.2	0.01
	Cu2 (4)	$\frac{1}{4}$	$\frac{1}{2}$	$a\sqrt{2}/2$	0.0636	3.2	3.2	−6.4	0.00
	O1 (4)	$\frac{1}{8}$	$\frac{1}{8}$	$3a/2$	0.0038	14.2	−8.8	−5.4	0.24
	O2 (8)	$\frac{1}{8}$	$\frac{3}{8}$	$a\sqrt{5}/2$	0.0089	14.5	−8.8	−5.7	0.22
	O3 (4)	$\frac{3}{8}$	$\frac{3}{8}$	$a/2$	0.0139	15.0	−8.9	−6.1	0.19
0.167	Cu1 (2)	0	$\frac{1}{4}$	$a\sqrt{10}/2$	0.0591	3.0	2.8	−5.8	0.02
	Cu2 (4)	$\frac{1}{3}$	$\frac{1}{4}$	$a\sqrt{2}/2$	0.0730	3.5	3.5	−7.0	0.01
	O1 (4)	$\frac{1}{6}$	$\frac{1}{4}$	$a\sqrt{5}/2$	0.0087	14.7	−9.0	−5.7	0.22
	O2 (2)	$\frac{1}{2}$	$\frac{1}{4}$	$a/2$	0.0195	15.5	−9.1	−6.4	0.18
	O3 (1)	0	$\frac{1}{2}$	$3a/2$	0.0079	14.6	−9.0	−5.6	0.23
	O4 (2)	$\frac{1}{3}$	$\frac{1}{2}$	$a/2$	0.0165	15.3	−9.1	−6.2	0.19
	O5 (1)	0	0	$a\sqrt{13}/2$	0.0084	14.7	−9.0	−5.7	0.23
	O6 (2)	$\frac{1}{3}$	0	$a\sqrt{5}/2$	0.0121	14.9	−8.9	−6.0	0.20
0.22	Cu1 (1)	0	0	$a\sqrt{2}/2$	0.0863	3.6	3.9	−7.5	0.04
	Cu2 (4)	$\frac{1}{3}$	0	$a\sqrt{2}/2$	0.0853	4.0	3.8	−7.8	0.02
	Cu3 (2)	$\frac{1}{3}$	$\frac{1}{3}$	$a\sqrt{2}/2$	0.0775	3.6	3.6	−7.2	0.01
	Cu4 (2)	$\frac{2}{3}$	$\frac{1}{3}$	$a\sqrt{10}/2$	0.0757	3.4	3.4	−6.8	0.00
	O1 (4)	$\frac{1}{6}$	0	$a/2$	0.0253	15.7	−9.2	−6.6	0.16
	O2 (2)	$\frac{1}{2}$	0	$a\sqrt{5}/2$	0.0166	15.0	−9.0	−6.0	0.19
	O3 (4)	$\frac{1}{3}$	$\frac{1}{6}$	$a/2$	0.0241	15.6	−9.2	−6.4	0.17
	O4 (4)	$\frac{2}{3}$	$\frac{1}{6}$	$a\sqrt{5}/2$	0.0164	15.1	−9.1	−6.0	0.21
	O5 (4)	$\frac{1}{2}$	$\frac{1}{3}$	$a\sqrt{5}/2$	0.0151	15.0	−9.1	−5.9	0.21
0.25	Cu1 (4)	$\frac{1}{4}$	$\frac{1}{4}$	$a\sqrt{2}/2$	0.0858	4.0	3.9	−7.9	0.01
	O1 (4)	$\frac{1}{4}$	0	$a\sqrt{5}/2$	0.0190	15.4	−9.0	−6.4	0.17
	O2 (4)	$\frac{1}{2}$	$\frac{1}{4}$	$a/2$	0.0218	15.7	−9.1	−6.6	0.16

in the two upper rows of the figure. $\delta=0.125$ and $\delta=0.25$ give rise to tetragonal cells with $2\sqrt{2}\times 2\sqrt{2}$ and 2×2 single cell volumes, respectively; all other structures are orthorhombic.

The charge of a given site calculated within the supercell approach results from the influence of all dopant ions which may be generally long-ranged. However, due to the two-dimensional character of the carriers in the high-T_c cuprates, the interaction of the dopant with its surrounding is screened at an in-plane length scale which is approximately the distance between the dopant and the CuO_2 plane.[14] Hence this interaction is short-ranged. Therefore the sizes of the chosen supercells are big enough to study the effects of charge redistribution caused even by a single dopant ion. The fact that the doping-induced charges averaged over the respective unit cell are only very weakly sensitive to the choice of the supercell has already been pointed out in Ref. 6. In order to get more insight into the effects on the local environment, we consider an alternative supercell for $\delta=0.25$ as given in the lowest panel of Fig. 1. This structure exhibits a less homogeneous distribution of dopants. Since it, however, is energetically unfavorable, as will be discussed below, the corresponding structural data and results are not displayed in Table I.

All calculations have been carried out within the DFT employing the full-potential linearized augmented plane-wave (LAPW) method utilizing the WIEN2K code.[15] Exchange and correlation effects were treated within the local density approximation. Atomic-sphere sizes of 2.0, 2.2, 1.9, and 1.55 were taken for Hg, Ba, Cu, and O, respectively. The k-point mesh was chosen such that for all structures the density of k points was the same or very similar. For comparison, the corresponding mesh for the single cell consists of $12\times 12\times 6$ points in the full Brillouin zone. Self-consistency was obtained such that for all symmetry-decomposed charges the fluctuations between two iterations were smaller than 10^{-4} electrons, and the total energies were converged better than 0.1 mRy. Due to the heavy computational effort, the crystal lattices have not been relaxed, but the doping-dependent crystalline data have been taken from Ref. 16. However, as inferred from similar calculations for $YBa_2Cu_3O_{6+x}$ with various doping contents,[7] we are confi-

dent that the lattice relaxation near the dopant ions will only moderately affect our findings.

III. RESULTS

A. Charge distribution

The atomiclike basis functions used within the LAPW method inside the so-called atomic spheres[17,18] allow us to analyze the charge density within each sphere by decomposing it with respect to the contributions of different orbital characters. Although these numbers depend on the choice of the atomic-sphere radii they provide useful information about the charges around different atomic sites.

The decrease in the partial charges in the atomic spheres averaged over the respective unit cells have been described in detail in Ref. 6. It was observed that a linear increase in the total number of holes for $\delta \leqslant 0.22$ is followed by a plateau at higher δ. The reason for this saturation was found in the fact that at $\delta \approx 0.22$ the dopant reaches a closed shell O^{2-} configuration. The ratio of the additional average hole contents on Cu($d_{x^2-y^2}$) and O(p_x) orbitals $h_{\mathrm{Cu}}/h_{\mathrm{O}}$ is approximately 4.0. (Note that there are two oxygen atoms in the CuO_2 plane per chemical formula unit, therefore the amount of oxygen holes is half that of copper.)

Now we focus on the charge distribution on the atomic scale. The presence of the dopant atom makes the atomic sites chemically inequivalent, and depending on the doping level the CuO_2 $pd\sigma$ bands experience a splitting with respect to the undoped case. Accordingly, the partial charges, densities of states, and electric field gradients may substantially differ from each other.

Table I presents the number of holes h_s created at the specific copper and oxygen sites in the CuO_2 planes with the undoped material taken as the reference. As one can see, h_s strongly depends on the atomic species, the specific site, and the doping content. Concerning the doping dependence, for all given δ values lower than 0.25, the maximal difference in the number of doping-induced holes among nonequivalent sites of the same species (denoted as $\Delta h_s^{\max}$) is approximately $0.01e$, although the distances from the ions to the next dopant may be quite different at smaller doping concentrations. For a fixed doping content, we define a measure for the inhomogeneity $\Delta h_s^{\max}$ divided by the average doping-induced charge of this species, i.e., h_{Cu} or h_{O}. This value decreases for copper from 21% for $\delta=0.125$ to 13% for $\delta=0.22$ (and zero for $\delta=0.25$). For oxygen it is much more pronounced with values of 114%, 95%, 51%, and 14% for $\delta=0.125$, 0.167, 0.22, and 0.25, respectively. Summarizing these findings we conclude that the relative inhomogeneity with respect to the total amount of doping-induced holes (i) is more pronounced for oxygen than for copper, since doping introduces less holes on the oxygen than on the copper sites, and (ii) is decreasing with increasing δ.

The isotropy of the charge distribution for $\delta=0.25$ given in the table may be considered as an artifact due to the choice of the supercell. For this reason, we have performed calculations for an alternative structure, which is displayed in the lowest panel of Fig. 1. For this case, the inhomogeneity is slightly more pronounced, with $\Delta h_s^{\max}=0.013$ for copper, still being in the range of a hundredth of an electron as found for the other doping concentrations. But more important, the total energy of this structure is more than 5 mRy per formula unit higher, which corresponds to a temperature of about 900 K. This large energy compared to the other cell choice can be explained by the smaller distance between the nearest neighbor dopants, which, being highly negatively charged, repel each other. For the other doping concentrations, we have chosen the supercells such that the separation of dopants is maximal.

The nonuniform charge distribution can also be understood in terms of the distances to the next dopant ion. Focusing on the projection onto the CuO_2 plane the spacings to the copper positions are $a\sqrt{2}/2$, $a\sqrt{10}/2$, etc. Although for all δ values the maximum amount of holes at Cu is created in the first coordination shell with the distance being $a\sqrt{2}/2$, its value strongly depends on δ. While for $\delta=0.125$ and 0.167 there are only two nonequivalent copper positions differing in the distance to the dopant, there are four nonequivalent Cu atoms for $\delta=0.22$. In this case, the biggest amount of holes is created at Cu1, which is influenced by two dopant sites with the same distance; Cu2 exhibits the same spacing to the nearest dopant atom, but the next nearest dopant oxygen is farther away. A similar analysis can be done for the oxygen sites, where the in-plane distances to the dopant are $a/2$, $a\sqrt{5}/2$, $3a/2$, etc. For example, at $\delta=0.125$, O3 (at a distance of $a/2$) is most affected by the excess oxygen, followed by O2, which interacts with a dopant at a distance of $a\sqrt{5}/2$, and O1 where the dopant is $3a/2$ away. Also for the oxygen sites the amount of created holes very strongly depends on the oxygen concentration, when positions with the same spacing to the dopant are compared. The values for the nearest dopant range from 0.0139 for $\delta=0.125$ via 0.0195 for $\delta=0.167$ to 0.0241 for $\delta=0.22$.

The valence charges can be related to the position of the corresponding core states. Analyzing the O-1s core levels with respect to the Fermi energy, we find that they move up with higher oxygen concentration. The average energy is -36.8186 Ry for $\delta=0.125$ and -36.8065 for $\delta=0.25$. For a fixed doping level, the variation of the 1s energies among the different oxygen sites is roughly 0.01 Ry. The higher the core state is in energy, the lower is the corresponding hole content. This situation reflects the antibonding character of the oxygen valence states. For all oxygen concentrations, the position of the dopant is about 0.05–0.06 Ry higher in energy than those of the plane oxygens, which experience a strong covalent bond with their copper neighbors. Looking at the Cu core levels, their variation in energy for a given δ is much less pronounced.

B. Electric field gradients

The distribution of doping-induced charges can be probed by nuclear quadrupole and magnetic resonance. The electronic and nuclear charge densities form a nonuniform electric field within the unit cell. A nuclear quadrupole moment is coupled to the gradients of the electric field[19] given by $V_{\alpha\beta}=\partial E_\alpha/\partial x_\beta$, where E_α is the component of the local electric field, and x_β is the Cartesian coordinate. The traceless

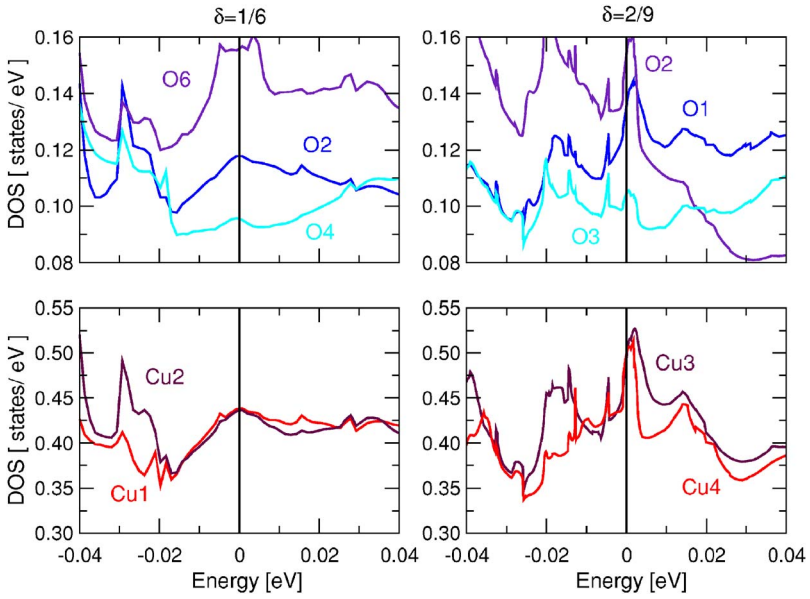

FIG. 2. (Color online) Selected Cu($d_{x^2-y^2}$) and O(p_x) contributions to the density of states in states per eV stemming from the respective atomic spheres for two different doping concentrations. The vertical lines indicate the Fermi level.

tensor $V_{\alpha\beta}$ can be diagonalized and written in the principal axes as $V_{\gamma\gamma}$. The isotopes ^{17}O and ^{63}Cu are usually used as the probes of electric field gradients in high-T_c cuprates. As a result of the interaction of their nuclear quadrupole momenta Q with the electric field gradients at the lattice sites, a resonance line at

$$\omega = \frac{eQ}{2\hbar} V_{zz}(1 + \eta^2/3)^{1/2} \tag{1}$$

appears in the radio frequency wave absorption spectrum of the system. Ordering the tensor elements by their absolute value, such that V_{xx} is the smallest and V_{zz} is the maximal component, the asymmetry parameter η is defined as $(V_{xx} - V_{yy})/V_{zz}$, where V_{zz} is called *the* electric field gradient EFG. The corresponding tensor components and asymmetry parameters are given in Table I. Some of the site symmetries give rise to nondiagonal components, which are, however, very small. Therefore, the principle tensor axes nearly coincide with the crystal axes and thus $V_{\gamma\gamma}$ are given as the corresponding diagonal elements. Recent experimental data[12] on EFGs in $La_{2-x}Sr_xCuO_4$ clearly show the following observations: There is (i) a doping-induced upward shift of the mean copper EFG in the order of 10%, (ii) a splitting of the resonance line according to different inequivalent sites, and (iii) a decrease in the splitting of the resonant frequencies of two different Cu sites with increasing doping. As one can conclude from Table I, all these findings are consistent with our results.[20] NMR measurements on Tl-based compounds[11] exhibit changes in the Cu and O EFGs of the order of 10% with doping, again concomitant with our calculations. At the same time, NQR data taken on Hg1202 also revealed an upward shift with doping,[21] which is, however, too large in order to be understood in terms of oxygen-doping induced holes only. We suppose additional defects[22,23] to be responsible for such a strong increase of the resonant frequencies. Our results are in a good qualitative agreement with the experimental observations of Ref. 24 performed on under- and overdoped $HgBa_2CuO_{4+\delta}$ crystals. In these measurements, a shift, a splitting, and a change of the in-plane ^{17}O NMR linewidth were revealed with the change of the doping concentration.

C. Density of states

Having discussed the site-dependent properties, we turn our attention to the density of states (DOS), which is an integral characteristic of the system and should be crucial for the transition temperature. In Fig. 2, the site-projected densities of states are presented for δ=0.167 and 0.22, highlighting the contributions of selected copper and oxygen spheres. Like the charge carriers, the DOS's also exhibit pronounced inhomogeneities which are of a similar order of magnitude. The relative differences in the DOS at the Fermi level from different oxygen sites are up to roughly 70% in both cases, while these are much smaller for the copper spheres. For δ =0.167 the two values are nearly the same, while the differences are somewhat bigger for δ=0.22, where the smallest and largest contribution are 0.468 (not shown in the figure) and 0.500, respectively. This feature is much more pronounced when moving away from the Fermi level in the range of 0.05 eV which is a typical energy scale of quasiparticles mediating the pairing. At δ=0.167 all contributions show broad peaks at the same energy which is slightly below the Fermi level. For δ=0.22 the peaks have become much sharper and have moved somewhat above E_F. Again, all copper and oxygen contributions exhibit their maxima at the same position.

Although charges and densities of states demonstrate similarities, which are inhomogeneities of the same order of magnitude, there is a clear difference in their behavior when we focus on the DOS in the vicinity of the Fermi level. This comes from the fact that the charges are obtained by integrals of the DOS over the whole valence energy range. Yet, only a small energy range around E_F is relevant for superconductivity. A noticeable fact in this context is that upon doping the $pd\sigma$ band becomes less populated, which is important for the charges in the CuO_2 plane. Regarding the DOS at E_F, also

the position of the saddle point (often referred to as a van Hove singularity) with respect to the Fermi level plays a role.

IV. CONCLUSIONS

To summarize, we have performed *ab initio* calculations for the oxygen-doped $HgBa_2CuO_4$ to consider inhomogeneity effects on the charges and densities of states. We find pronounced differences in the doping-induced number of holes at given copper and oxygen sites, where the degree of the inhomogeneity strongly depends on the doping level and the atomic species. Our results are consistent with the findings of Pan *et al.*[9] giving a spatial scale of a few lattice parameters. Furthermore, they explain the behavior of NMR and NQR lines, i.e., a shift and a splitting with doping.[11,12,21]

Besides the atomic-scale experiments discussed above, there could be further consequences of the nonuniform charge distribution on larger spatial scales. This distribution gives rise to a random potential for the carriers near the Fermi level leading to their momentum relaxation. On the macroscopic scale, these effects have been seen in the resistivity measurements[26] and electronic Raman spectroscopy.[25] In a $d_{x^2-y^2}$ superconductor, such a potential is pair-breaking and leads to a reduction of T_c. This decrease, however, turned out to be smaller than expected from the momentum relaxation rate, as it was shown in Ref. 27. On the nanoscale, this random potential leads to the electron inhomogeneity for the low-energy states probed by the scanning tunneling spectroscopy in the superconducting state.[10,28–30]

Concerning the density of states, which is directly connected to superconductivity, we observe that the contributions of all plane copper and oxygen species are different in magnitude but peak at the same energy. Going below and above E_F we find more pronounced differences which makes us conclude that the importance of the inhomogeneities for superconductivity strongly depends on the energy and character of the quasiparticle mediating the Cooper pairing.

ACKNOWLEDGMENTS

This work was supported by the Austrian Science Fund, Projects No. P13430, No. P14004, and No. M591. One of us (E.Y.S.) is grateful to A. Balatsky for valuable discussion and interest in this work.

*Electronic address: cad@mu-leoben.at

[1] S. N. Putilin, E. V. Antipov, O. Chmaissem, and M. Marezio, Nature (London) **362**, 226 (1993).
[2] D. L. Novikov and A. J. Freeman, Physica C **212**, 233 (1993).
[3] D. J. Singh, Phys. Rev. B **48**, 3571 (1993).
[4] D. L. Novikov and A. J. Freeman, Physica C **216**, 273 (1993).
[5] D. J. Singh and W. E. Pickett, Phys. Rev. Lett. **73**, 476 (1994).
[6] C. Ambrosch-Draxl, P. Süle, H. Auer, and E. Ya. Sherman, Phys. Rev. B **67**, 100505(R) (2003).
[7] C. Ambrosch-Draxl, P. Khorzhavyi, and B. Johansson (unpublished).
[8] J. M. Tranquada, in *Neutron Scattering in Layered Copper-Oxide Superconductors*, edited by A. Furrer (Kluwer, Dordrecht, The Netherlands, 1998), p. 225.
[9] S. H. Pan, J. P. ONeal, R. L. Badzey, C. Chamon, H. Ding, J. R. Engelbrecht, Z. Wang, H. Eisaki, S. Uchida, A. K. Gupta, K. W. Ng, E. W. Hudson, K. M. Lang, and J. C. Davis, Nature (London) **413**, 282 (2001).
[10] K. McElroy, J. Lee, J. A. Slezak, D.-H. Lee, H. Eisaki, S. Uchida, and J. C. Davis, Science **309**, 1048 (2005).
[11] A. Gerashenko, Yu. Piskunov, K. Mikhalev, A. Ananyev, K. Okulova, S. Verkhovskii, A. Yakubovskii, L. Shustov, and A. Trokiner, Physica C **328**, 163 (1999).
[12] P. M. Singer, A. W. Hunt, and T. Imai, cond-mat/0302078 (unpublished).
[13] Z. Wang, J. R. Engelbrecht, S. Wang, H. Ding, and S. H. Pan, Phys. Rev. B **65**, 064509 (2002).
[14] T. Ando, A. B. Fowler, and F. Stern, Rev. Mod. Phys. **54**, 437 (1982).
[15] P. Blaha, K. Schwarz, G. K. H. Madsen, D. Kvasnicka, and J. Luitz, WIEN2K, An Augmented Plane Wave + Local Orbitals Program for Calculating Crystal Properties (Vienna University of Technology, Vienna, 2001).
[16] Q. Huang, J. W. Lynn, Q. Xiong, and C. W. Chu, Phys. Rev. B **52**, 462 (1995).
[17] D. J. Singh, *Planewaves, Pseudopotentials and the LAPW Method* (Kluwer Academic Publishers, Boston, 1994).
[18] C. Ambrosch-Draxl, Phys. Scr., T **109**, 48 (2004).
[19] M. H. Cohen and F. Reif, in *Quadrupole Effects in Nuclear Magnetic Resonance Studies of Solids*, edited by Seitz and Turnbull, Solid State Physics, Vol. 5 (Academic Press, New York, 1957).
[20] The EFG on the plane copper atom turned out to be typically underestimated by a factor of 2 compared to experiments [K. Schwarz, C. Ambrosch-Draxl, and P. Blaha, Phys. Rev. B **42**, 2051 (1990)]. Nevertheless the trends are reproduced correctly.
[21] A. A. Gippius, E. V. Antipov, W. Hoffmann, and K. Lüders, Physica C **276**, 57 (1997).
[22] O. Chmaissem, J. D. Jorgensen, D. G. Hinks, J. L. Wagner, B. Dabrowski, and J. F. Mitchell, Physica C **241-243**, 805 (1998).
[23] E. V. Antipov, A. M. Abakumov, and S. N. Putilin, Supercond. Sci. Technol. **15**, 31 (2002).
[24] J. Bobroff, H. Alloul, P. Mendels, V. Viallet, J.-F. Marucco, and D. Colson, Phys. Rev. Lett. **78**, 3757 (1997).
[25] Y. Gallais, A. Sacuto, and D. Colson, Physica C **408-410**, 785 (2004).
[26] A. Yamamoto, W.-Z. Hu, and S. Tajima, Phys. Rev. B **63**, 024504 (2001).
[27] H.-Y. Kee, Phys. Rev. B **64**, 012506 (2001).
[28] K. McElroy, R. W. Simmonds, J. E. Hoffman, D.-H. Lee, J. Oresnstein, H. Eisaki, S. Uchida, and J. C. Davis, Nature (London) **422**, 592 (2003).
[29] K. M. Lang, V. Madhavan, J. E. Hoffman, E. W. Hudson, H. Eisaki, S. Uchida, and J. C. Davis, Nature (London) **415**, 412 (2002).
[30] G. Kinoda, T. Hasegawa, S. Nakao, T. Hanaguri, K. Kitazawa, K. Shimizu, J. Shimoyama, and K. Kishio, Phys. Rev. B **67**, 224509 (2003).